Biogeosciences Discuss., doi:10.5194/bg-2015-613, 2016
Manuscript under review for journal Biogeosciences
Published: 18 January 2016

Mechanisms of *Trichodesmium* bloom demise within the New Caledonia Lagoon during the VAHINE mesocosm experiment

D. Spungin[1], U. Pfreundt[2], H. Berthelot[3], S. Bonnet[3,4], D. AlRoumi[5], F. Natale[5], W.R. Hess[2], K.D. Bidle[5], I. Berman-Frank[1]

[1] {The Mina and Everard Goodman Faculty of Life Sciences, Bar-Ilan University, Ramat-Gan, Israel}
[2] {University of Freiburg, Faculty of Biology, Schänzlestr. 1, D-79104 Freiburg, Germany}
[3] {Aix Marseille Université, CNRS/INSU, Université de Toulon, IRD, Mediterranean Institute of Oceanography (MIO) UM 110, 13288, Marseille, France}
[4] {Institut de Recherche pour le Développement (IRD), AMU/CNRS/INSU, Université de Toulon, Mediterranean Institute of Oceanography (MIO) UM 110, 13288, Marseille-Noumea, France-New Caledonia}
[5] {Department of Marine and Coastal Sciences, Rutgers University, New Brunswick, NJ, USA}

Correspondence to: I. Berman-Frank (ilana.berman-frank@biu.ac.il)

Biogeosciences Discuss., doi:10.5194/bg-2015-613, 2016
Manuscript under review for journal Biogeosciences
Published: 18 January 2016

Abstract

The globally important marine diazotrophic cyanobacterium *Trichodesmium* blooms regularly in the New Caledonian lagoons (Sowthwestern Pacific). We exploited the development of a *Trichodesmium* bloom in the lagoon waters outside the enclosed VAHINE mesocosms to specifically investigate the cellular processes mediating its decline. *Trichodesmium* cells (and associated microbiota) were sampled from the time of surface accumulation to biomass demise using a series of enclosed incubations to elucidate the stressors and subcellular underpinning of rapid (~ 24 h) biomass demise and disappearance. The development and decline of *Trichodesmium* populations was rapid with extensive surface accumulations (blooms) appearing within 24 h on the surface waters of the lagoon. Rapid decline of > 90 % biomass after 24 h of peak accumulation was observed in populations that were collected and incubated under ambient conditions. Metatranscriptomic profiling of *Trichodesmium* biomass 8 h and 22 h after bottle incubation of surface accumulations revealed evidence for phosphorus (P) and iron (Fe) stress, with upregulation of genes required to increase their availability and transport. In contrast, genes responsible for nutrient storage were downregulated. Total viral abundance, assessed by SYBR-green staining and analytical flow cytometry, oscillated throughout the experiment and showed no significant relationship with *Trichodesmium* bloom development or demise. Enhanced caspase-specific activity and upregulation of a suite of metacaspase genes during bloom demise implicated autocatalytic programmed cell death (PCD) as the mechanistic cause. At the same time, genes associated with buoyancy and gas-vesicle production were strongly downregulated concomitant with high concentrations of transparent exopolymeric particles (TEP), greatly aiding aggregation and expediting vertical flux to depth. Our results demonstrate that the rapid demise of this high-density, *Trichodesmium* surface bloom over 24 h was not caused by specific lytic infection but was rather induced by PCD in response to combined nutrient and oxidative stressors.

Biogeosciences Discuss., doi:10.5194/bg-2015-613, 2016
Manuscript under review for journal Biogeosciences
Published: 18 January 2016

1 Introduction

The New Caledonia lagoon in the southwestern Pacific Ocean is characterized by abundant blooms of the filamentous, diazotrophic (N_2-fixing) cyanobacterium *Trichodesmium* spp. that appear regularly during austral summer conditions between December and March (Dandonneau and Gohin, 1984; Dupouy et al., 2011). *Trichodesmium* spp. are important contributors to marine N_2 fixation as they form massive oceanic blooms throughout the oligotrophic marine sub-tropical and tropical oceans (Capone and Carpenter, 1982; Capone et al., 1997; Capone et al., 2004). These surface blooms with densities of 2 x 10^8 cells L^{-1} develop swiftly and are characterized by high rates of CO_2 and N_2 fixation (Capone et al., 1998; Rodier and Le Borgne, 2008; Luo et al., 2012).

Trichodesmium has been extensively investigated [reviewed in Capone et al. (1997); and Bergman et al. (2012)], yet relatively few publications have examined the mortality and fate of these blooms that often collapse abruptly with mortality rates paralleling growth rates (Rodier and Le Borgne, 2008; Rodier and Le Borgne, 2010; Bergman et al., 2012). Mortality of blooms can be induced by grazing of *Trichodesmium* by pelagic harpacticoid copepods (O'Neil, 1998) or from viral lysis (Hewson et al., 2004). *Trichodesmium* can also die via genetically controlled programmed cell death (PCD) induced by nutrient (iron (Fe) starvation) or oxidative stress in both laboratory and natural populations (Berman-Frank et al., 2004; Berman-Frank et al., 2007; Bar-Zeev et al., 2013). Mortality of *Trichodesmium* via PCD results in distinct morphologically and physiological characteristics and triggers rapid sinking of biomass that may influence carbon export in oligotrophic environments (Bar-Zeev et al., 2013). Sinking is due to concomitant internal cellular degradation, vacuole loss, and the increased production of extracellular polysaccharide aggregates, operationally defined as transparent exopolymeric particles (TEP) (Berman-Frank et al., 2004; Berman-Frank et al., 2007; Bar-Zeev et al., 2013).

Our initial objective during the VAHINE project (Bonnet et al., This issue-b) was to study the involvement of PCD in the fate of natural *Trichodesmium* blooms induced within large (~ 50 m^3) mesocosms in the New Caledonia Lagoon and followed over the course of several weeks. While *Trichodesmium* was initially present and conditions in the mesocosms appeared favorable, no *Trichodesmium* blooms developed within the mesocosms with other diazotrophs (such as diatom-diazotroph associations, and unicellular types mainly UCYN-C, as well as UCYN-A and UCYN-B) instead developing and dominating at different phases of the

Biogeosciences Discuss., doi:10.5194/bg-2015-613, 2016
Manuscript under review for journal Biogeosciences
Published: 18 January 2016

experimental period (Turk-Kubo et al., 2015). Here, we exploited a short-lived *Trichodesmium* bloom that developed and crashed outside the mesocosms (in the lagoon waters) toward the end of the VAHINE experiment. Using a series of microcosm incubations with collected *Trichodesmium* biomass, we elucidated the stressors and subcellular underpinning of rapid (~ 24 h) biomass demise and disappearance. Here we present, for the first time, *in-situ* physiological, biochemical, and metatranscriptomic evidence for nutrient and oxidative stress-induced PCD that lead to the *Trichodesmium* bloom crash and, combined with concomitant downregulation of gas vesicles and enhanced TEP production, was coupled with export flux.

2 Methods

2.1. Sampling site and sampling conditions during pre-bloom periods

Our study was performed during the VAHINE mesocosm project set 28 km off the coast of New Caledonia from 13 January 2013 (day 1) to 6 February 2013 in the New Caledonia oligotrophic lagoon at (22°29.10' S, 166° 26.90' E). The 25 m deep sandy-bottom lagoon is generally protected from the dominant trade winds yet the waters of the lagoon are influenced by the oligotrophic oceanic waters coming into the lagoon via the Boulari Pass (Bonnet et al., This issue-b). Detailed descriptions of the site selection and sampling strategy are provided elsewhere (Bonnet et al., This issue-b). The lagoon waters outside the enclosed mesocosms were sampled daily during the experiment and serve as 'pre-bloom' data. Large volume samples (50 L) were collected from 1, 6, and 12 m depths at 07:00 h using a Teflon® PFA pump and PVC tubing. Samples were immediately transferred back to laboratories aboard the R/V Alis and subsampled for a suite of parameters [as described below and in Bonnet et al. (This issue-b)]. On day 23 at 12:00 h, a large surface accumulation of *Trichodesmium* was observed in the lagoon close to the enclosed mesocosms. This biomass accumulation (hereafter called – "bloom") served as the source for subsequent experiments and investigations into its fate (detailed below).

2.2. Short-term incubations to assess bloom decline

Experiment 1- *Trichodesmium* filaments and colonies were collected from the dense surface bloom (day 23, 12:00 h; designated $T_{0,}$ Fig. 2a-c) using a plankton net (mesh size, 80 µm) from the surface water. The total contents of the net were resuspended in six identical 4.5 L Nalgene polycarbonate bottles (Fig. 2d-e) containing 0.2 µm pore size, filtered sea water (FSW) and incubated as detailed below. **Experiment 2-** Seawater from the surface bloom was

Biogeosciences Discuss., doi:10.5194/bg-2015-613, 2016
Manuscript under review for journal Biogeosciences
Published: 18 January 2016

collected 5 h after the initial surface bloom was sighted (day 23, 17:00; designated T_5) by directly filling 20 L polyethylene carboys, gently to avoid destroying biomass. Bottles from experiments 1 and 2 were placed in on-deck in incubators filled with running seawater to maintain ambient surface temperature (~ 26 °C) and covered with neutral screening at 50 % surface irradiance levels. Water from experiment 1 was sampled every 2-4 h until the biomass collapsed (after ~ 22 h) for: Chl *a* concentration, caspase activity, 16S rRNA gene sequencing, and metatranscriptomics. Water from experiment 2 was sampled for PON, POC, NH_4^+, N_2 fixation rates, TEP production, and virus abundance (days 23-25).

2.3. Chlorophyll a concentrations

Samples for the determination of chlorophyll *a* (Chl *a*) concentrations during pre-bloom days were collected by filtering 550 mL of seawater on GF/F filters. Filters were directly stored in liquid nitrogen. Chl *a* was extracted in methanol and measured fluorometrically (Herbland et al., 1985). During short-term experiment 1, samples for Chl *a* were collected by filtering 200 mL on GF/F filters (Whatman, Kent, UK). Chl *a* was extracted in methanol and measured spectrophotometrically (664 and 750 nM; CARY100, Varian, Santa Clara, CA, USA) according to Tandeau de Marsac and Houmard (1988).

2.4. Determination of particulate organic carbon (POC) and nitrogen (PON) during pre-bloom conditions

Detailed POC analyses are described in Berthelot et al. (2015). Samples were collected by filtering 2.3 L of seawater through pre-combusted (450 °C, 4 h) GF/F filter and determined using the combustion method (Strickland and Parsons, 1972) on an EA 2400 CHN analyzer. Samples for PON concentrations were collected by filtering 1.2 L of water on pre-combusted (450 °C, 4 h) and acid washed (HCl, 10 %) GF/F filters and analyzed according to the wet oxidation protocol described in Pujo-Pay and Raimbault (1994) with a precision of 0.06 µmol L^{-1}.

2.5. N_2 fixation rates and NH_4^+ concentrations

N_2 fixation rates measurements used in experiment 2 are described in details in (Berthelot et al., 2015). Samples were collected in 4.5 L polycarbonate bottles and amended with $^{15}N_2$-enriched seawater according to the protocol developed by Mohr et al. (2010) and (Rahav et al., 2013). Seawater was degassed through a degassing membrane (Membrana, Minimodule®, flow rate fixed at 450 mL min^{-1}) connected to a vacuum pump. Degassed seawater was

Biogeosciences Discuss., doi:10.5194/bg-2015-613, 2016
Manuscript under review for journal Biogeosciences
Published: 18 January 2016

amended with 1 mL of $^{15}N_2$ (98.9 % atom % ^{15}N, Cambridge isotope) per 100 mL. The bottle was shaken vigorously and incubated overnight at 3 bars at to promote $^{15}N_2$ dissolution. Incubation bottles were amended with 1:20 (vol:vol) of $^{15}N_2$-enriched seawater, closed without headspace with silicone septum caps, and incubated for 24 h under *in situ*-simulated conditions in on-deck incubators (described above). 2.2 L from each experimental bottle were filtered under low vacuum pressure (< 100 mm Hg) onto a pre-combusted (450 °C, 4 h) GF/F filter (25 mm diameter, 0.7 µm nominal porosity) and the filters stored at -20 °C until analysis, then dried for 24 h at 60 °C before mass spectrometric analysis. PON content and PON ^{15}N enrichments were determined using a Delta plus Thermo Fisher Scientific isotope ratio mass spectrometer (Bremen, Germany) coupled with an elemental analyzer (Flash EA, Thermo Fisher Scientific). N_2 fixation rates were calculated according to the equations detailed in Montoya et al. (1996). Rates were considered significant when the ^{15}N enrichment of the PON was higher than three times the standard deviation obtained from T_0 samples.

Samples for NH_4^+ were collected in 40 mL glass vials and analyzed by the fluorescence method according to Holmes et al. (1999), using a Trilogy fluorimeter (Turner Design).

2.6. Transparent exopolymeric particles (TEP)

Water samples (100 mL) were gently (<150 mbar) filtered through a 0.45 µm polycarbonate filter (GE Water & Process Technologies). Filters were then stained with a solution of 0.02 % Alcian blue (AB), 0.06 % acetic acid (pH of 2.5), and the excess dye was removed by a quick deionized water rinse. Filters were than immersed in sulfuric acid (80 %) for 2 h, and the absorbance (787 nm) was measured spectrophotometrically (CARY 100, Varian). AB was calibrated using a purified polysaccharide gum xanthan (GX) (Passow and Alldredge, 1995). TEP concentrations (µg GX equivalents L^{-1}) were measured according to (Passow and Alldredge, 1995).

2.7. Virus abundance

Total seawater (1 mL) was fixed with 0.5 % glutaraldehyde and snap frozen in liquid N_2 until processed. Flow cytometry was conducted using an Influx Model 209S Mariner flow cytometer and high-speed cell sorter equipped with a 488 nm 200 mW blue laser, 4 way sort module, 2 scatter, 2 polarized and 4 fluorescence detectors (BD Biosciences). Viral abundance was determined by staining fixed seawater samples with SYBR Gold (Life Technologies) and measurements of green fluorescence (520 nm, 40 nm band pass). Samples were thawed, diluted 25-fold in 0.22 µm-filtered Tris/EDTA (TE) buffer (pH 8), stained with SYBR Gold

(0.5 - 1X final concentration), incubated for 10 min at 80°C in the dark, cooled to RT for 5 min, and mixed thoroughly by vortexing prior to counting on the Influx (Brussaard, 2003). Viral abundance was analyzed using a pressure differential (between sheath and sample fluid) of 0.7, resulting in a low flow rate for higher event rates of virus like particles counts.

2.8. Caspase activity

Biomass was collected on 25 mm, 5 µm pore-size polycarbonate filters and resuspended in 0.6-1 mL Lauber buffer [50 mM HEPES (pH 7.3), 100 mM NaCl, 10 % sucrose, 0.1 % 3-(3-cholamidopropyl)-dimethylammonio-1-propanesulfonate, and 10 mM dithiothreitol] and sonicated on ice (four cycles of 30 seconds each) using an ultra-cell disruptor (Sonic Dismembrator, Fisher Scientific, Waltham, MA, USA). Cell extracts were centrifuged (10,000 x *g*, 2 min, room temperature) and supernatant was collected for caspase biochemical activity. Caspase-specific activity was determined by measuring the kinetics of cleavage for the canonical fluorogenic caspase substrate (Z-IETD-AFC) at a 50 mM final concentration (using Ex400 nm, Em505 nm; Synergy4 BioTek, Winooski, VT, USA), as previously described in Bar-Zeev et al. (2013). Fluorescence results were converted to a normalized substrate cleavage rate using an AFC standard (Sigma). Caspase activity rates were normalized to total protein concentrations.

2.9. 16S rRNA gene sequencing and data analyses

Bacterial community diversity was analyzed by deep sequencing of the 16S rRNA gene in samples from two replicate bottles from experiment 1 (see section 1.2) at three time points each. Seawater samples were filtered on 25 mm, 5 µm pore-size Supor filters (Pall Gelman Inc., Ann Arbor, Michigan), snap frozen in liquid nitrogen, and stored at -80 °C for later extraction. Community genomic DNA was isolated from the filters using a phenol–chloroform extraction method modified according to Massana et al. (1997). The 16S rRNA genes within community genomic DNA were initially amplified with conserved bacterial primers 27F and 1100R (Dowd et al., 2008) using a high fidelity polymerase (Phusion DNA polymerase, Thermo Scientific) with an initial denaturation step of 95 ºC for 3 min followed by 20 cycles of 95 ºC for 30 sec, 55 ºC for 30 sec, and 72 ºC for 45 sec. A secondary PCR (same conditions) was performed for next-generation sequencing (Ion Torrent™ Life Technologies, USA) by using customized fusion primers with different tag sequences. The tags were attached to the 27F primer and to the 338R primer (Hamady et al., 2008) to obtain 340 bp fragments suitable for IonTorrent analysis. The use of nested PCR was used to minimize

Biogeosciences Discuss., doi:10.5194/bg-2015-613, 2016
Manuscript under review for journal Biogeosciences
Published: 18 January 2016

inclusion of false sequences into the sequenced material (Dowd et al., 2008). After secondary PCR all amplicon products were purified using Ampure magnetic purification beads (Agencourt Bio- science Corporation, MA, USA) to exclude primer-dimers. The amplicons were sequenced at the Bar-Ilan Sequencing Center.

The adapter-clipped sequences were processed using tools and scripts from the UPARSE pipeline (Edgar, 2013). Sequences were de-multiplexed, primers and barcodes stripped using the script *fastq_strip_barcode_relabel.py*, leaving 42747 raw reads altogether for six samples. As suggested for single-end amplicon sequences, sequences (mostly between 280 nt and 300 nt) were trimmed to a fixed length of 280 nt, and shorter sequences were discarded (26740 trimmed raw reads remaining). For OTU clustering, trimmed raw reads were quality filtered using the *–fastq_filter* command with a maximum expected error rate (*-fastq_maxee*) of two (21590 reads remaining), clustered into unicals (100 % identity) and the unicals sorted by weight (number of sequences in the cluster). OTU clustering with an identity threshold of 0.98 was done using the *-cluster_otus* command on sorted unicals, with built-in chimera filtering. The trimmed raw reads (after a more relaxed quality filtering with *-fastq_maxee* 5) were mapped back to these OTUs with *-usearch_global* and a minimum identity of 98 % to infer each OTUs abundance in each sample. For taxonomic classification, OTUs were submitted to https://www.arb-silva.de/ngs/ and classified using the SINA aligner v1.2.10 and database release SSU 123 (Quast et al., 2013). Sequences having a (*BLAST alignment coverage* + *alignment identity*)/2 < 93 % were considered as unclassified and assigned to the virtual taxonomical group "No Relative" (5.58 % of OTUs).

2.10. RNA extraction and metatranscriptome sequencing

Metatranscriptomic sequencing was performed for three time points: peak surface accumulation of the bloom (T_0), 8 h (T_8), and 22 h (T_{22}) after T_0. Cells on polycarbonate filters were disrupted by adding 1 mL PGTX [for 100 mL final volume: phenol (39.6 g), glycerol (6.9 mL), 8-hydroxyquinoline (0.1 g), EDTA (0.58 g), sodium acetate (0.8 g), guanidine thiocyanate (9.5 g), guanidine hydrochloride (4.6 g) and Triton X-100 (2 mL)] (Pinto et al, 2009) and 250 µl glass beads (diameter 0.1 – 0.25 mm) in a cell disruptor (Precellys, Peqlab, Germany) for 3 x 15 s at 6500 rpm. Tubes were placed on ice between each 15 s interval. RNA was extracted by adding 0.7 mL chloroform and subsequent phase separation. RNA was precipitated from the aqueous phase using 3 vol isopropanol at -20 °C overnight. Residual DNA was removed using the Turbo DNA-free Kit (Ambion) after the

Biogeosciences Discuss., doi:10.5194/bg-2015-613, 2016
Manuscript under review for journal Biogeosciences
Published: 18 January 2016

manufacturer's instructions, but adding additional 1 µl of DNase after 30 min of incubation and incubating another 30 min. RNA was purified using Clean & Concentrator 5 columns (Zymo Research, Freiburg, Germany). The pure RNA was treated with Ribo-Zero rRNA Removal Kit (Bacteria) (Epicentre, Madison, USA) and purified again. DNA contamination was tested with a 40 cycle PCR using cyanobacteria-specific 16S primers.

For removal of tRNAs and small fragments, the RNA was purified with the Agencourt RNAClean XP kit (Beckman Coulter Genomics, Danvers, USA). First-strand cDNA synthesis for T_8 and T_{22} samples was primed with a N6 randomized primer, after which the cDNAs were fragmented with ultrasound (4 pulses of 30 sec at 4°C). Illumina TruSeq sequencing adapters were ligated to the 5' and 3' ends and the resulting cDNAs were PCR-amplified to about 10-20 ng μL^{-1} using a high fidelity DNA polymerase. Randomly-primed cDNA for T_0 samples was prepared using purified RNA without fragmentation followed by ligation of Illumina TruSeq sequencing adapters to the 5' and 3' ends and fragmentation with ultrasound (4 pulses of 30 sec at 4°C; targeting only cDNA > 700 nt). After repairing ends, dA-tailed and Illumina TruSeq sequencing adapters were ligated again to the 5' and 3' ends of the cDNA and then re-amplified. Consequently, a small fraction of the T_0 reads was not strand-specific. All cDNAs were purified using the Agencourt AMPure XP kit (Beckman Coulter Genomics, Danvers, USA) and 2 x 150 nt paired-end sequences generated with an Illumina NextSeq500 sequencer by a commercial provider (vertis AG, Freising, Germany).

2.11. Bioinformatics processing and analysis of metatranscriptome data

To remove adapters, perform quality trimming, and set a minimal length cutoff, raw fastq reads were processed with Cutadapt version 1.8.1 (Martin, 2011) in paired-end mode with a minimum adapter sequence overlap of 10 nt (-O 10), an allowed error rate of 20 % (-e 0.2) in the adapter sequence alignment, and a minimum base quality of 20. To remove residual ribosomal RNA reads, the fastq files were further processed with SortMeRNA version 1.8 (Kopylova et al., 2012) with the accompanying standard databases in paired end mode, resulting in 9,469,339 non-ribosomal reads for T_0, 22,407,194 for T_8, and 18,550,250 for T_{22}. The fastq files with all non-ribosomal forward-reads were used for mapping against the *Trichodesmium erythraeum* IMS101 genome with Bowtie2 (Langmead and Salzberg, 2012) in *very-sensitive-local* mode. This resulted in 51.9 % of T_0, 5.1 % of T_8, and 3.3 % of T_{22} reads mapped. Reads were counted per CDS feature as annotated in the genome of *Trichodesmium*

Biogeosciences Discuss., doi:10.5194/bg-2015-613, 2016
Manuscript under review for journal Biogeosciences
Published: 18 January 2016

erythraeum (NC_008312.1) using htseq-count version 0.6.0 (Anders et al., 2014) and a count table generated with all read counts from T_0, T_8, and T_{22}.

For detection of differentially expressed genes from T_0 to T_8 and T_8 to T_{22}, the count table was processed with the statistical tool "Analysis of Sequence Counts" (ASC) (Wu et al., 2010), which estimates the posterior probabilities (P) of genes > 2-fold differentially expressed (user specified threshold) between any two samples using an empirical Bayesian analysis algorithm and a normalization step. Differential expression of genes was defined as significant if P > 0.98.

3 Results

3.1. Bloom development and biomass demise.

Within the duration of the VAHINE experiment, the total Chl *a* concentrations in the lagoon ranged between 0.18 to 0.25 µg L^{-1} from days 1 to 15, 0.24–0.26 µg L^{-1} from days 16 through 20, and by the morning of day 23 Chl *a* increased to 0.39 µg L^{-1} in the upper 1m depth (Fig 1). The increase in Chl *a* concentrations reflect the composite signature of the total phototrophic community detailed in (Van Wambeke et al., This issue; Leblanc et al., This issue) and is not specific to *Trichodesmium* biomass. Low abundances of *Trichodesmium* were measured in the lagoon waters throughout the first three weeks of the project (Turk-Kubo et al., 2015), with *Trichodesmium*-associated 16S counts ranging from 0.1 to 0.4 % of the total number of 16S tags (Pfreundt et al., This issue). During the first eight days of sampling, *Trichodesmium* abundance ranged between 3.4 x 10^2 - 6.5 x 10^3 *nifH* copies L^{-1}. By days 14 and 16. *Trichodesmium* contribution accounted for 15 % of the total diazotroph population (with 1.1-1.5 x 10^4 *nifH* copies L^{-1}) while by day 22 *nifH* copies L^{-1} increased further to 1.4 x 10^5 *nifH* copies L^{-1} (Turk-Kubo et al., 2015).

Dense surface accumulations of *Trichodesmium* were observed at midday (12:00 h) on day 23 (February 4), when ambient air temperatures increased to 26 ºC and the winds decreased to < 5 knots (Fig. 2a-c). These blooms appeared in the typical "slick" formations with dense surface biomass spread out over tens of meters in the lagoon waters outside the mesocosm (Fig. 2a-c). The spatially patchy nature of *Trichodesmium* blooms in the lagoon (Fig. 2a-c), and the rapid temporal modifications in cellular density induced by turbulence and wind-stress, complicate *in-situ* sampling that targets changes in a specific biomass when it is not enclosed. Thus, to investigate the mechanisms determining cell fate, we specifically collected the *Trichodesmium* bloom populations, resuspended them in replicate bottles (Fig. 2d-e), and

Biogeosciences Discuss., doi:10.5194/bg-2015-613, 2016
Manuscript under review for journal Biogeosciences
Published: 18 January 2016

followed temporal changes during two short-term experiments (see methods). Based on previous experience (Berman-Frank et al., 2004), resuspension of *Trichodesmium* cells in the extremely high densities of the surface blooms (Fig. 2a-c) would cause an almost immediate crash of the biomass. Consequently, we resuspended the collected biomass in FSW at lower cell densities so as to not induce this artifact. The dominance of *Trichodesmium* spp. as the almost sole autotrophic representative (see later Fig. 4) in these bottles enabled the use of Chl *a* to follow changes in its biomass (Fig 2f). The highest Chl *a* concentrations (> 150 ± 80 µg L^{-1}; n=6) were measured at noon (12:00 h) on day 23 within accumulated, surface-bloom patches. In these incubations, *Trichodesmium* populations collapsed swiftly over the next day with Chl *a* concentrations declining to 24 µg L^{-1} and 11 µg L^{-1} Chl *a* after 10 and 22 h, respectively (Fig. 2f).

N_2 fixation rates ranged between 0.09-1.2 nmol N L^{-1} h^{-1} during the pre-bloom period (Fig. 3a) and were 0.5 nmol L^{-1} h^{-1} during sampling on day 23 (Fig. 3a). High respective rates of N_2 fixation (3.5 ± 2.8 nmol N L^{-1} h^{-1} and 11.7 ± 3.4 nmol N L^{-1}) were measured during the *Trichodesmium* crash after 13 and 29 h, respectively (Fig. 3b). Notably, these high values may represent other diazotrophs that flourished after *Trichodesmium* biomass had declined. PON, which represents the fraction of N incorporated into biomass, ranged between 0.6 µmol L^{-1} to 1.8 µmol L^{-1} during pre-bloom periods (Fig. 3a). PON respectively increased to 5 ± 3.6 µmol L^{-1} and doubled to 10 ± 3.3 µmol L^{-1} 17 and 44 h after biomass accumulation (Fig. 3b). Leakage of NH_4^+ and dissolved organic N (DON) is common during the process of N_2 fixation in *Trichodesmium* (Mulholland and Capone, 2000). NH_4^+ in seawater is also commonly regenerated from organic nitrogen by bacterial remineralization. The NH_4^+ concentrations during pre-bloom periods ranged between 17 to 50 nmol L^{-1} (Fig. 3c) and increased to 73 ± 0.0004 nmol L^{-1} 5 h after bloom accumulation (17:00 h) (Fig. 3d). Forty-two hours after the *Trichodesmium* biomass collapsed, NH_4^+ concentrations rose exponentially with values > 5000 nmol L^{-1}, representing a 70-fold increase compared to pre-bloom and bloom concentrations (Fig. 3d).

3.2. Associated microbial and viral communities

The microbial community associated with the *Trichodesmium* bloom was analyzed from two replicate bottles from short-term experiment 1. During the peak of the bloom, 94 % and 93 % of the obtained 16S tags in both replicates (Fig. 4) were of the *Oscillatoriales* order (Phylum-Cyanobacteria), with 99.9 % of these sequences classified as *Trichodesmium* spp. (Fig. 4). In

both bottles, a decline of *Trichodesmium* coincided with an increase in *Alteromonas* 16S tags, but this development lagged in replicate 1 compared to replicate 2 (Fig. 4). Six hours (T_6) after the surface bloom was originally sampled (T_0), 80 % of 16S tags from replicate 1 were still *Trichodesmium*, while they had declined to ~ 20 % in replicate 2. *Trichodesmium* was replaced by *Alteromonadales* and *Vibrionales* in replicate 1 (represented by only 9 % of 16S tags) after 13 h and was not detectable in replicate 2, instead being comprised predominantly by *Alteromonadales* at this time.

Virus like particles (VLP) ranged between 1 to 6 x 10^6 mL^{-1} throughout the first 22 days of VAHINE and displayed a ~ 2-4 day oscillation (i.e., increasing for 2 d, then declining for the next 3 days, etc.) with mean values of 3.8 x 10^6 ± 1.7 mL^{-1} (Fig. 5a). VLP counts in surface waters on day 23 were 1.8 x 10^6 mL^{-1} (Fig. 5a), just prior to the appearance of the surface bloom. VLPs did not show any distinct correlations with total biomass indices such as POC and PON during both the pre-bloom sampling and short-bloom experiments (Fig. 5a-b). By the time the surface bloom of *Trichodesmium* was sampled, VLPs abundance was at a maximum of 8 x 10^6 mL^{-1} (Fig. 5b), declining slightly in the next 5 h, and remaining relatively stable throughout the crash period (within the next 24 h) averaging ~ 5 x 10^6 ± 0.7 mL^{-1} (Fig. 5b).

3.3. Environmental stressors (Fe, P)

During the VAHINE experiment, depth-averaged DIP concentrations in the lagoon waters were 0.039 ± 0.001 µM, with a relatively stable DIP turnover time (T_{DIP}) of 1.8 ± 0.7 d for the first 15 days, which declined by day 23 to 0.5 ± 0.7 d (Berthelot et al., 2015). Alkaline phosphatase activity (APA), which hydrolyzes inorganic phosphate from organic phosphorus, increased ~ 5 fold between values at the start of the experiment 0.71 ± 0.18 (day 2) to 5.0 ± 0.1 nmole L^{-1} h^{-1} (average of days 20-23) (Van Wambeke et al., This issue) demonstrating the decreasing availability of DIP in the lagoon waters and a response in metabolic activity related to P acquisition for the microbial community**.**

The density of *Trichodesmium* filaments and colonies within the bottle incubation experiments was maintained lower than the *in situ* densities found in the intense surface accumulations; yet the Chl a concentrations of ~ 150 ± 80 µg L^{-1} were still ~ 500 fold higher than that measured in the water just prior to the surface accumulation (Fig. 1 and Fig. 2f). While we did not directly determine nutrient concentrations within the surface patches, it would be reasonable to assume that nutrient pressure on these dense surface populations (i.e. competition for and

Biogeosciences Discuss., doi:10.5194/bg-2015-613, 2016
Manuscript under review for journal Biogeosciences
Published: 18 January 2016

utilization rates) exceeded that in the bottles. Growth of *Trichodesmium* is inhibited when T_{DIP} < 2 d, (Moutin et al., 2005). Yet, *Trichodesmium* is able to obtain phosphorus from both DIP, and organic P sources, including methylphosphonate, ethylphosphonate, and 2-aminoethylphosphonate (Dyhrman et al., 2006; Beversdorf et al., 2010). Genes involved in the acquisition and transport of inorganic and organic P sources were upregulated, concomitant with biomass demise; higher expression levels were observed at T_8 and T_{22} compared to T_0 (Table S1). Abundance of alkaline phosphatase transcripts, encoded by the *phoA* gene (Orchard et al., 2003), increased significantly (by ~ 5 fold) from T_0 (178 RPM) to T_{22} (885 RPM) (Fig. 6a). Additionally, the transcript abundance of phosphonate transporters and C-P lyase genes (*phnC, phnD, phnE, phnH, phnI, phnL and phnM*) increased significantly (5-12 fold) between T_0 and both T_8 and T_{22} (Fig 6a; Table S1).

Three arsenate reductases genes, encoded by *arsA*, exist in the *T. erythraeum* genome. Transcripts of all three were detected in the metatranscriptome data. Maximal transcripts were measured for two *arsA* genes at T_0 with subsequent declines (Tery_0013 by 50 % from 1556/1466 RPM at T_0 and T_8 to 768 RPM at T_{22}; Tery_2327 by almost 80 % from 1275 RPM at T_0 to 397 RPM and 291 RPM at T_8 and T_{22}, respectively; Table S1). The third *arsA* gene (Tery_0875) was not differentially expressed in the metatranscriptome data (Table S1).

The *isiB* gene encodes for flavodoxin and serves as a common diagnostic indicator of Fe stress in *Trichodesmium*, since it may substitute for Fe-S containing ferredoxin (Chappell and Webb, 2010; Bar-Zeev et al., 2013). *isiB* transcripts were significantly higher at T_0 (3-fold) than at T_8 and T_{22} (Fig. 6b, Table S1), indicative of Fe stress at the time of maximal biomass accumulation in the surface waters. The Fe transporter gene *idiA* showed a transient higher transcript accumulation only at T_8. As *Trichodesmium* mortality progressed the transcripts of the Fe storage gene, ferritin (*Dps*) decreased by > 70 % T_{22} (Fig. 6b, Table S1). The chlorophyll-binding protein, IsiA, is induced in cyanobacterial species under Fe and oxidative stress to prevent oxidative damage (Laudenbach and Straus, 1988). Here, *isiA* transcripts increased 2- and 3-fold from T_0 to T_8 and T_{22}, respectively, yet not significantly (Fig. 6b, Table S1).

3.4. PCD-induced demise.

We employed two independent biomarkers to investigate PCD induction during *Trichodesmium* bloom demise, namely changes in catalytic rates of caspase-specific activity and levels of metacaspase transcript expression. When the surface bloom was sampled (T_0),

protein normalized, caspase-specific activity was 0.23 ± 0.2 pmol mg protein^{-1} min^{-1} (Fig. 7a). After a slight decline in the first 2 h, caspase activities increased throughout the experiment with 10 fold higher values (2.9 ± 1.5 pmol L^{-1} mg protein^{-1} min^{-1}) obtained over the next 22 h as the bloom crashed (Fig. 7a).

The dynamics of transcript expression was analyzed for the 12 identified metacaspase genes within *Trichodesmium* [(Berman-Frank et al., 2004; Asplund-Samuelsson et al., 2012; Asplund-Samuelsson, 2015); *TeMC1* (Tery_2077), *TeMC2* (Tery_2689), *TeMC3* (Tery_3869), *TeMC4* (Tery_2471), *TeMC5* (Tery_2760), *TeMC6* (Tery_2058), *TeMC7* (Tery_1841), *TeMC8* (Tery_0382), *TeMC9* (Tery_4625), *TeMC10* (Tery_2624), *TeMC11* (Tery_2158), and *TeMC12* (Tery_2963)], a subset of which were previously implicated in PCD of *Trichodesmium* cultures in response to Fe and light stress (Berman-Frank et al., 2004; Bar-Zeev et al., 2013; Bidle, 2015). Here, we expanded our analysis to interrogate the entire suite of metacaspases in natural populations. As the biomass crashed from T_0 to T_{22}, eight out of twelve metacaspases, including all highly expressed ones (> 1000 RPM), were upregulated with significant changes in expression occurring mainly during the first 8 hours of the experiment (between T_0 to T_8) (Fig. 7b, Table S1). Transcript abundances increased between 2.5-fold and 8-fold for these genes. Of the lower expressed genes (< 400 RPM), three were amongst the significantly upregulated ones, and three were not differentially expressed. *TeMC12* was not expressed throughout the experiment.

3.5. Export flux

Our earlier studies showed that PCD-induced demise in *Trichodesmium* is characterized by an increase in the amount of excretion and concentrations of TEP, (Berman-Frank et al., 2007) and sinking of particulate organic matter (Bar-Zeev et al., 2013). During the pre-bloom period (first 20 days), TEP concentrations in the lagoon waters fluctuated around ~ 350 µg gum xanthan (GX) L^{-1}. With the higher *Trichodesmium* biomass, TEP concentrations increased to ~ 500 µg GX L^{-1} on day 22 (Fig. 8a). TEP concentration exceeded 700 GX L^{-1} on day 23 during the collapse of the bloom (4 h to 20 h after T_0) and then declined to 420 GX L^{-1} 44 h after T_0 (Fig. 8b). The corresponding POC concentrations ranged between ~ 5.2 and 11.2 µmol L^{-1} during pre-bloom periods (Fig. 8a). Within the bloom, POC increased to 18-29 µmol L^{-1} 9 to 25 h after sightings of the surface bloom and peaked towards the end of the incubation experiment reaching 66 µmol L^{-1} after 45 h; this represented a 10 fold increase over pre-bloom periods (Fig. 8b). Export flux can be enhanced by PCD-induced sinking (Bar-Zeev et al.,

Biogeosciences Discuss., doi:10.5194/bg-2015-613, 2016
Manuscript under review for journal Biogeosciences
Published: 18 January 2016

2013) as PCD in *Trichodesmium* also results in the collapse of internal components, especially gas vesicles that are required for buoyancy (Berman-Frank et al., 2004). Although we did not measure changes in buoyancy, the metatranscriptomic analyses demonstrated that, excluding one copy of *gvpL/gvpF*, encoding a gas vesicle synthesis protein, gas vesicle protein *(gvp)* genes involved in gas-vesicle formation *(gvpA, gvpN, gcpK, gvpG and gvpL/gcpF)* were all significantly downregulated relative to T_0 (Fig. 9, Table S1).

4 Discussion

4.1. *Trichodesmium* bloom development and crash

Warm (25-30 °C) and stable water columns with low turbulence are ideal conditions for *Trichodesmium* to accumulate on the sea surface of the New Caledonian lagoon (Rodier and Le Borgne, 2008). Thus, the high temperatures of the lagoon waters ~ 26 °C, and reduced wind speeds < 5 knots were conducive to the observed surface accumulations. These dense aggregations were typical for the frequent austral-summer *Trichodesmium* blooms within the New Caledonia lagoon (Dandonneau and Gohin, 1984; Dupouy et al., 2000; Rodier and Le Borgne, 2008; Rodier and Le Borgne, 2010). Phytoplankton blooms and their phenotypic dense surface accumulations occur under favorable physical properties of the upper ocean (e.g. temperature, mixed-layer depth, stratification) and specifically when division rates exceed loss rates derived from grazing, viral attack, and sinking or export from the mixed layer to depth (Behrenfeld, 2014). In the South Pacific, the massive *Trichodesmium* blooms often collapse abruptly with mortality rates similar to growth rates (Rodier and Le Borgne, 2008; Rodier and Le Borgne, 2010). Although physical drivers such as turbulence and mixing may scatter and dilute these dense accumulations, their rapid disappearance (within 3-5 d) suggests loss of biomass by other mechanisms. Here, we specifically focused on the loss factors, and show the involvement of biotic and abiotic stressors inducing PCD and thereby mechanistically affecting the fate of *Trichodesmium* biomass and the bloom demise.

4.2. Community dynamics

Under conditions of high biomass accumulation of filaments and colonies *Trichodesmium* will respond to nutrient dynamics and cell signaling, as well as to community interactions between *Trichodesmium* cells, grazers, and viruses. *Trichodesmium* is grazed by harpacticoid copepods of the *Miraciidae* family, mostly by *Macrosetella*, (O'Neil and Roman, 1994; O'Neil, 1998). Zooplankton counts of harpacticoids during the days of the large surface accumulations of

Biogeosciences Discuss., doi:10.5194/bg-2015-613, 2016
Manuscript under review for journal Biogeosciences
Published: 18 January 2016

Trichodesmium yielded ~ 20 individuals m^{-3} thereby refuting the possibility that these would cause the massive decline (Hunt et al., This issue). A wide diversity of microorganisms are found closely associated with *Trichodesmium* colonies, including specific epibionts, viruses, bacteria, eukaryotic microorganisms and metazoans (Paerl et al., 1989; Siddiqui et al., 1992; Zehr, 1995; Ohki, 1999; Sheridan et al., 2002; Hewson et al., 2009; Hmelo et al., 2012).

Although for the first three weeks of the experiment *Trichodesmium* comprised a < 1 % fraction of the 16S tags (Pfreundt et al. this issue) and *nifH* transcript abundance ranged between 3.4 x 10^2 - 6.5 x 10^3 *nifH* copies L^{-1} (d 2-18) (Turk-Kubo et al., 2015), its rapid development and high biomass on day 23 established its role as a keystone species that greatly influences the system. At the time of the surface bloom, *Trichodesmium* dominated the collected biomass with more than 90 % of all 16S tags sequenced (Fig. 4). As the *Trichodesmium* biomass declined, very high concentrations of NH_4^+ were measured in the incubation bottles (> 5000 nmol L^{-1}) (Fig. 3d). *Trichodesmium* can release up to 50–80 % of their recently fixed N_2 as $NH4^+$ and DON (Mulholland, 2007), which can sustain both autotrophic and heterotrophic organisms (Berthelot et al., 2015; Bonnet et al., This issue-a). Additionally, the high DOC and high TEP concentrations rich in organic C, measured during bloom collapse (Fig. 8b) (Berman-Frank et al., 2007), must have stimulated and supported the observed rapid growth of *Alteromonas* species within the γ-Proteobacteria (Fig. 4). *Alteromonas sp.* are known 'copiotrophs', organisms equipped to capitalize on nutrient and carbon rich environments (Ivars-Martinez et al., 2008). *Alteromonas* and other γ-Proteobacteria appear frequently associated with *Trichodesmium* colonies under bloom conditions (Hewson et al., 2009) and their proliferation during biomass collapse confirms their reputation as fastidious and opportunistic microorganisms (Allers et al., 2008; Hewson et al., 2009). Associated epibiont bacterial abundance in laboratory cultures (Spungin et al., 2014) and in rapidly growing populations of *Trichodesmium* is relatively limited compared to that observed during bloom decline (Hewson et al., 2009; Hmelo et al., 2012). Once PCD or other stressors negatively impact *Trichodesmium* growth, opportunists such as *Alteromonas or Vibrionales* (Pichon et al., 2013; Frydenborg et al., 2014) can thrive on the influx of organic nutrient sources from the decaying *Trichodesmium* (Fig. 4) and enhance the recycling of organic matter in the upper water layers, reducing C-export and further impact the biogeochemical cycling of C and N (Hmelo et al., 2011).

Viruses have been increasingly invoked as key agents terminating phytoplankton blooms (Tarutani et al., 2000; Jacquet et al., 2002; Brussaard et al., 2005; Vardi et al., 2012; Lehahn et

al., 2014). In *Trichodesmium*, phages have been implicated in bloom crashes, but this mechanism has yet to be unequivocally proven (Ohki, 1999; Hewson et al., 2004); indeed, no specific *Trichodesmium* phage has been isolated or characterized to date (Brown et al. 2013). Here, total VLP abundance, was highest at maximum surface accumulation of *Trichodesmium* biomass and was generally steady at ~ 5-6 x 10^6 VLPs mL^{-1} during bloom demise. While our method of analysis cannot distinguish between phages infecting *Trichodesmium* from other marine bacteria, it argues against a massive, phage-induced lytic event of *Trichodesmium*. Such an event would have yielded a notable burst of VLPs upon bloom crash, especially considering the high *Trichodemsium* biomass observed. The coincidence between the highest VLPs and highest *Trichodesmium* biomass is counter to viruses serving as the mechanism of mortality in our incubation experiments. Nonetheless, virus infection itself may be a stimulant for community N_2 fixation perhaps by releasing key nutrients (i.e., P or Fe) upon lysis of surrounding microbes. Although we could not identify them, it is indeed possible that *Trichodesmium*-specific phages were present in our incubation experiments and they may have exerted additional physiological stress on resident populations, facilitating PCD induction. Virus infection increase the cellular production of reactive oxygen species (ROS) (Evans et al., 2006; Vardi et al., 2012), which in turn can stimulate PCD in algal cells (Berman-Frank et al., 2004; Thamatrakoln et al., 2012; Bidle, 2015). Viral attack can also directly trigger PCD as part of an antiviral defense system to limit virus production and prevent massive viral infection (Georgiou et al., 1998; Bidle and Falkowski, 2004; Bidle, 2015).

4.3. Nutrient Stress

Dense blooms of *Trichodesmium* with high requirements for inorganic Fe (Kustka et al., 2002) may experience reduced Fe availability that could induce stress responses including PCD. Although the new Caledonian lagoon is considered Fe replete (Latham, 1981), in the dense surface accumulations, the physiological requirements of *Trichodesmium* fixing N_2 and C create a high demand for macro- and micro-nutrients, such as P and Fe reducing their bioavailability. Our data from the short-term incubation experiments with dense *Trichodesmium* populations shows that *Trichodesmium* responded to DIP limitation over a 22 h period after surface biomass accumulation by inducing a 5-fold increase of *phoA* transcripts, required for APA to hydrolyze inorganic phosphate from organic phosphorus (Orchard et al., 2003) (Fig. 6a).

Biogeosciences Discuss., doi:10.5194/bg-2015-613, 2016
Manuscript under review for journal Biogeosciences
Published: 18 January 2016

Trichodesmium can also utilize organic molecules with C-P bond (phosphonates) (Dyhrman et al., 2002; Dyhrman et al., 2006; Beversdorf et al., 2010; Hove-Jensen et al., 2014) and has eleven respective genes contained within the *phn*DCEEGHIJKLM operon (Hove-Jensen et al., 2014). Our data shows enhanced expression of *phnD, phnC, phnE, phnH, phnI, phnJ, phnK, phnL* and *phnM* (Fig. 6a, Table S1) that are consistent with previous results demonstrating that *phnD* and *phnJ* expression levels increased during DIP depletion (Hove-Jensen et al., 2014). *Trichodesmium's* ability to utilize methylphosphonate, ethylphosphonate, and 2-aminoethylphosphonate as DIP sources (Beversdorf et al., 2010) is apparently driven by a modified and un-elucidated C-P lyase pathway that differs from *E. coli* and other *phnP* and *phnN*-containing organisms (Hove-Jensen et al., 2014). Furthermore, the phosphonate ABC transporter genes *phnC-E* are duplicated in *Trichodesmium* and may have functionally diverged, a possible explanation for their differing transcript abundances during bloom demise (Fig. 6a and Table S1). As *Trichodesmium* has the capacity for using multiple P sources (Dyhrman et al., 2006; Beversdorf et al., 2010), it is likely that during bloom demise, the C-P lyase pathway of remaining living cells was induced when DIP sources were extremely low while POP and DOP increased with the decaying organic matter. The ability to use phosphonates as a P source can provide a competitive advantage for phytoplankton and bacteria in P-depleted waters (Coleman and Chisholm, 2010; Martinez et al., 2010). Thus, it is puzzling why dying cells would upregulate genes such as *phn* genes. A more detailed temporal-resolution of the metatranscriptomic analyses may elucidate the dynamics of these genes and their regulating factors. Alternatively, in PCD-induced populations, a small percentage remains viable and resistant as either cysts (Vardi et al., 1999) or hormogonia (Berman-Frank et al., 2004) that can serve as the inoculum for future blooms. It is plausible that the observed upregulation signal was attributable to these sub-populations.

When DIP concentrations are low, coupling between arsenate uptake and P utilization can occur (Cutter and Cutter, 2006; Dyhrman and Haley, 2011). Arsenate, which is toxic for most organisms, interferes with enzyme function and serves as a phosphate analog disrupting phosphate uptake and utilization (Dyhrman and Haley, 2011). In oligotrophic regions, arsenate may be transported into cells through phosphate uptake systems (Hewson et al., 2009), thus requiring cellular resistance strategies to ameliorate the toxic effects. One of these cellular strategies allows the reduction of arsenate to arsenite, which is followed by the removal of arsenite from the cell through the arsenite efflux pumps encoded by *arsA* and *arsB* genes (Dyhrman and Haley, 2011). *Trichodesmium* possesses the arsenate reductase gene *arsA*, but

Biogeosciences Discuss., doi:10.5194/bg-2015-613, 2016
Manuscript under review for journal Biogeosciences
Published: 18 January 2016

not *arsB*. Here, two out of three *arsA* genes in *Trichodesmium* (Tery_0013 and Tery_2327) were highly expressed especially during the peak of the bloom and their expression declined by ~ 50 % and ~ 80 % at T_{22} when most biomass had crashed (Table S1). Active *arsA* expression in *Trichodesmium* populations from the south Pacific has been noted previously (Hewson et al. 2009). Our data may indicate that inadvertent arsenate uptake during P-stress can also contribute another stress that could catalyze or induce bloom demise. This hypothesis remains to be validated.

While Fe availability is not typically limiting in the New Caledonia lagoon (Jacquet et al., 2006), we detected enhanced cellular Fe demand during the bloom crash using several proxy genes (Table S1). *Trichodesmium*'s strategies of obtaining and maintaining sufficient Fe involves genes such as *isiB*, which encodes for the flavin-containing flavodoxin to replace ferredoxin when Fe is limited (Leonhardt and Straus, 1992; La Roche et al., 1996; Chappell and Webb, 2010). *isiB* was highly expressed when biomass accumulated on the surface waters, indicative for higher Fe demand at this biomass load (Chappell and Webb, 2010; Bar-Zeev et al., 2013). High transcript abundance of this gene was also maintained throughout the bloom crash, albeit it was significantly downregulated, > 2-fold (Fig. 6b). Transcripts for chlorophyll binding Fe stress induced protein A (*IsiA*) increased (albeit not significantly) 3-fold over 22 h of bloom demise (Fig. 6b, Table S1). In many cyanobacteria, *isiA* expression is stimulated under Fe stress (Laudenbach and Straus, 1988) and oxidative stress (Jeanjean et al., 2003) and functions to prevent high-light induced oxidative damage by increasing cyclic electron flow around the photosynthetic reaction center photosystem I (Michel and Pistorius, 2004; Latifi et al., 2005; Havaux et al., 2005). Dense surface blooms of *Trichodesmium* are exposed to high irradiance (on day 23 average PAR was 3000 µmol photons m^{-2} s^{-1}) in the lagoon. Although we did not measure reduction of bioavailable Fe in the patches, it is possible that Fe consumption was high and combined with the oxidative stress of the high irradiance could was the high upregulate *isiA* (Fig. 6b). As cell density and associated self-shading of *Trichodesmium* filaments decreased during bloom crash, light-induced oxidative stress is likely the principal driver for elevated *isiA* expression.

Upregulated expression of *idiA* (an ABC Fe^{+3} transporter) was also observed over the first 8 h of bloom demise; *idiA* enables Fe to pass through the periplasm into the cytoplasm in bacteria and cyanobacteria (Chappell and Webb, 2010). This is consistent with increasing Fe-limitation, as *Trichodesmium* abundance (measured via 16S rRNA gene sequencing) remained high at T_8 after eight hours of dense *Trichodesmium* occurrence (replicate 1). Lastly, our

Biogeosciences Discuss., doi:10.5194/bg-2015-613, 2016
Manuscript under review for journal Biogeosciences
Published: 18 January 2016

metatranscriptomic data highlighted a reduction in Fe storage and utilization, as the expression of Fe-rich ferritin-like DPS proteins (Castruita et al., 2006), encoded by *dps*A, decreased ~ 5 fold by the time that most of the biomass crashed (T_{22}) (Fig. 6b, Table S1). *DpsA* was shown to be downregulated under Fe-replete conditions in *Synechococcus* (Mackey et al., 2015), but the downregulation observed here is more likely related to *Trichodesmium* cells dying and downregulating Fe-demanding processes such as photosynthesis and N_2 fixation.

4.4. Programmed cell death (PCD)

The physiological and morphological evidence of PCD in *Trichodesmium* has been previously documented in both laboratory (Berman-Frank et al., 2004; Bar-Zeev et al., 2013) and environmental cultures collected from surface waters around New Caledonia (Berman-Frank et al., 2004). Here, we confirmed characteristic features of *Trichodesmium* PCD associated with cell stress, such as increased caspase-specific activity (Fig. 7a), globally enhanced metacaspase expression (Fig. 7b), decreased expression of gas vacuole maintenance (Fig. 9), and higher TEP concentrations (Fig. 8b) in a naturally occurring *Trichodesmium* bloom *in situ*. Metatranscriptomic snapshots interrogating expression changes in all 12 *Trichodesmium* metacaspases (Fig. 7b) generally portrayed upregulated expression concomitant with biomass decline. Our results are consistent with previous observations that Fe-depleted PCD-induced laboratory cultures of *Trichodesmium* IMS101 had higher expression levels of *TeMC1* and *TeMC9* compared to healthy Fe-replete cultures (Berman-Frank et al., 2004; Bar-Zeev et al., 2013). To our knowledge, this is the first study examining expression levels of metacaspases in environmental *Trichodesmium* samples during a natural bloom. Eleven of the twelve annotated metacaspases in *Trichodesmium* were expressed in all three metatranscriptomes from the surface bloom with variability in expression levels likely reflecting structural and regulatory differences (Asplund-Samuelsson et al., 2012; Choi and Berges, 2013; Asplund-Samuelsson, 2015). To date, no specific function has been determined for any of these metacaspases in *Trichodesmium* other than their association with cellular stress and death. Efforts are underway to develop targeted functional genomics in order to elucidate the specific cellular functions, regulation, and protein interactions of these *Trhicodesmium* metacaspases (Pfreundt et al., 2014; Spungin et al., In prep).

In cultures and isolated natural populations of *Trichodesmium* high caspase-specific activity is correlated with the initial induction stages of PCD and activity subsequently declines as the

biomass crashes (Berman-Frank et al. 2004, 2007, Bar-Zeev et al. 2013). Here, caspase activity increased with the crashing populations of *Trichodesmium* (Fig 7a). Notably, maximal caspase activities were also observed at T_{23}, after which most *Trichodesmium* biomass had collapsed. The high protein-normalized caspase-specific activity may be a result of a very stressed and dying sub-population of *Trichodesmium* that had not yet succumbed to PCD (Berman-Frank et al. 2004). Alternatively, the high caspase activity could be attributed to the large population of *Altermomonas* bacteria that were associated with the remaining detrital *Trichodesmium* biomass. However, high cellular caspase-specific activity in clades of γ-Proteobacteria has yet to be published.

4.5. Export flux.

Gas vesicles are internal structures essential for maintaining buoyancy of *Trichodesmium* populations in the upper surface waters enabling them to vertically migrate and respond to light and nutrient requirements (Walsby, 1978; Capone et al., 1997). Mortality via PCD causes a decline in the number and size of cellular gas vesicles in *Trichodesmium* (Berman-Frank et al., 2004) and results in an enhanced vertical flux of trichomes and colonies to depth (Bar-Zeev et al., 2013). Our metatranscriptomic data supported the subcellular divestment from gas vesicles production during bloom decline, as the expression of vesicle-related genes were downregulated (Fig. 9). In parallel, TEP production and concentration increased to > 800 µg GX L^{-1}, a 2-fold increase from pre-bloom periods. When nutrient uptake is limited, but CO_2 and light are sufficient, uncoupling occurs between photosynthesis and growth (Berman-Frank and Dubinsky, 1999), leading to high production of the excess polysaccharides, such as TEP. This also corresponds to observations showing that the highest concentration of TEP occur during bloom decline phases rather than during the increase in populations (Smetacek, 1985; Engel, 2000).

In *Trichodesmium*, the contribution of the TEP pool to total DOC varies as a function of nutrient stress and enhances fluxes of organic matter (Berman-Frank et al., 2007; Bar-Zeev et al., 2013). Bloom collapse leads to the vertical export or recycling of newly fixed nitrogen and carbon in the ocean. In this case, TEP production has an important role in carbon fluxes in the ocean. Although TEP itself may be positively buoyant (Azetsu-Scott and Passow, 2004), its stickiness causes aggregation and clumping of cells and detritus, ultimately enhancing sinking rates of large aggregates and dying *Trichodesmium* (Bar-Zeev et al., 2013). The increasing TEP and aggregation of cellular debris probably stimulated the observed presence and growth of copiotrophs like *Alteromonas* and a greater degree of remineralization enriching these

microhabitats and the lagoon with high DOM, DOC, and inorganic nutrients that are available for other microorganisms. Thus, the increase in volumetric N_2 fixation and PON that was measured in the incubation bottles right after the *Trichodesmium* bloom crash probably reflects the enhanced activity of other diazotrophs and of resistant residual *Trichodesmium* trichomes or colonies (Berman-Frank et al. 2004) with increased cell specific N_2 fixation. This scenario is consistent with the hypothesis that PCD induction and death of a fraction of the population confers favorable conditions for survival and growth of individual cells (Bidle and Falkowski, 2004).

5 Conclusions

We demonstrate that the rapid demise of a *Trichodesmium* surface bloom in New Caledonia, with the disappearance of > 90 % of the biomass within < 24 h, displayed cellular responses to P and Fe stress and was mediated by a suite of PCD genes. Bloom crash does not appear to have been induced directly by virus infection and lysis, although virus infection may have modulated the cellular and genetic responses to enhance PCD-driven loss processes. Quorum sensing among epibionts (Van Mooy et al., 2012; Hmelo et al., 2012), allelopathic interactions, and the production of toxins by *Trichodesmium* (Guo and Tester, 1994; Kerbrat et al., 2010) are additional factors that could be important for a concerted response of the *Trichodesmium* population, yet we did not examine them here. Collectively, they would facilitate rapid collapse and loss of *Trichodesmium* populations, and possibly lead to enhanced vertical fluxes and export production, as previously demonstrated in PCD-induced laboratory cultures of *Trichodesmium* (Bar-Zeev et al., 2013). We posit that PCD induced demise, in response to concurrent cellular stressors, and facilitated by a concerted gene regulation, is typical in natural *Trichodesmium* blooms and leads to a high export production rather than regeneration and recycling of biomass in the upper photic layers.

Author contributions

Planning and conceptual framework of the bloom crash experiments was done by IBF, DS, and SB. DS, UP, HB, SB, WRH, KB and IBF all participated in the experimental sampling. DS, UP, HB, FN, DAR, KB, and IBF analyzed the samples and resulting data. IBF and DS wrote the manuscript with further contributions to the manuscript by UP, WRH, SB, and KB.

Acknowledgments

Funding was obtained for IBF through a collaborative grant from MOST Israel and the High Council for Science and Technology (HCST)-France, and a Binational Science Foundation grant (No: 2008048) to IBF and KB. This research was also funded in part by the Gordon and Betty Moore Foundation through Grant GBMF3789 to KDB. The participation of IBF, DS, UP, and WRH in the VAHINE experiment was supported by the German-Israeli Research Foundation (GIF), project number 1133-13.8/2011 and the metatranscriptome analysis by the EU project MaCuMBA (Marine Microorganisms: Cultivation Methods for Improving their Biotechnological Applications; grant agreement no: 311975) to WRH. Funding for VAHINE Experimental project was provided by the Agence Nationale de la Recherche (ANR starting grant VAHINE ANR-13-JS06-0002), INSU-LEFE-CYBER program, GOPS, IRD and M.I.O. The authors thank the captain and crew of the R/V Alis. We acknowledge the SEOH divers service from the IRD research center of Noumea (E. Folcher, B. Bourgeois and A. Renaud) and from the Observatoire Océanologique de Villefranche-sur-mer (OOV, J.M. Grisoni) as well as the technical service of the IRD research center of Noumea for their helpful technical support. Thanks especially to E. Rahav for his assistance throughout the New Caledonia experiment and to H. Elifantz for technical assistance with the 16S sequencing and data analysis. This work is in partial fulfillment of the requirements for a PhD thesis for D. Spungin at Bar-Ilan University.

References

Allers, E., Niesner, C., Wild, C., and Pernthaler, J.: Microbes enriched in seawater after addition of coral mucus, Applied and environmental microbiology, 74, 3274-3278, 2008.

Anders, S., Pyl, P. T., and Huber, W.: HTSeq–A Python framework to work with high-throughput sequencing data, Bioinformatics, btu638, 2014.

Asplund-Samuelsson, J., Bergman, B., and Larsson, J.: Prokaryotic caspase homologs: phylogenetic patterns and functional characteristics reveal considerable diversity, 2012.

Asplund-Samuelsson, J.: The art of destruction: revealing the proteolytic capacity of bacterial caspase homologs, Molecular Microbiology, 98, 1-6, 2015.

Azetsu-Scott, K., and Passow, U.: Ascending marine particles: Significance of transparent exopolymer particles (TEP) in the upper ocean, Limnol. & Oceanogr, 49, 741-748, 2004.

Bar-Zeev, E., Avishay, I., Bidle, K. D., and Berman-Frank, I.: Programmed cell death in the marine cyanobacterium *Trichodesmium* mediates carbon and nitrogen export, The ISME journal, 7, 2340-2348, 2013.

Behrenfeld, M. J.: Climate-mediated dance of the plankton, Nature Climate Change, 4, 880-887, 2014.

Bergman, B., Sandh, G., Lin, S., Larsson, J., and Carpenter, E. J.: *Trichodesmium* - a widespread marine cyanobacterium with unusual nitrogen fixation properties, FEMS Microbiol Rev, 1-17, 10.1111/j.1574-6976.2012.00352.x., 2012.

Berman-Frank, I., and Dubinsky, Z.: Balanced growth in aquatic plants: Myth or reality? Phytoplankton use the imbalance between carbon assimilation and biomass production to their strategic advantage, Bioscience, 49, 29-37, 1999.

Berman-Frank, I., Bidle, K., Haramaty, L., and Falkowski, P. G.: The demise of the marine cyanobacterium, *Trichodesmium* spp., via an autocatalyzed cell death pathway, Limnology and Oceanography, 49, 997-1005, 2004.

Berman-Frank, I., Rosenberg, G., Levitan, O., Haramaty, L., and Mari, X.: Coupling between autocatalytic cell death and transparent exopolymeric particle production in the marine cyanobacterium *Trichodesmium*, Environmental Microbiology, 9, 1415-1422, 10.1111/j.1462-2920.2007.01257.x, 2007.

Berthelot, H., Moutin, T., L'Helguen, S., Leblanc, K., Hélias, S., Grosso, O., Leblond, N., Charrière, B., and Bonnet, S.: Dinitrogen fixation and dissolved organic nitrogen fueled primary production and particulate export during the VAHINE mesocosm experiment (New Caledonia lagoon), Biogeosciences, 12, 4099-4112, 10.5194/bg-12-4099-2015, 2015.

Beversdorf, L., White, A., Björkman, K., Letelier, R., and Karl, D.: Phosphonate metabolism by *Trichodesmium* IMS101 and the production of greenhouse gases, Limnology and Oceanography, 55, 1768-1778, 2010.

Bidle, K. D., and Falkowski, P. G.: Cell death in planktonic, photosynthetic microorganisms, Nature Reviews Microbiology, 2, 643-655, 2004.

Bidle, K. D.: The molecular ecophysiology of programmed cell death in marine phytoplankton, Ann. Rev. Mar. Sci. , 7, in press, 2015.

Bonnet, S., Berthelot, H., Turk-Kubo, K., Fawcett, S., Rahav, E., Berman-Frank, I., and l'Helguen, S.: Dynamics of N_2 fixation and fate of diazotroph-derived nitrogen during the VAHINE mesocosm experiment (New Caledonia), This issue-a.

Bonnet, S., Helias, S., Rodier, M., Moutin, T., Grisoni, J. M., Louis, F., Folcher, E., Bourgeois, B., Boré, J. M., and Renaud, A.: Introduction to the project VAHINE: VAriability of vertical and trophic transfer of diazotroph derived N in the South West Pacific, This issue-b.

Brussaard, C. P. D., Mari, X., Van Bleijswijk, J. D. L., and Veldhuis, M. J. W.: A mesocosm study of Phaeocystis globosa (Prymnesiophyceae) population dynamics - II. Significance for the microbial community, Harmful Algae, 4, 875-893, 2005.

Brussaard, C. R. D.: Optimization of procedures for counting viruses by flow cytometry, App. Environ. Microbiol., 70, 1506-1513, 2003.

Capone, D., Burns, J., Montoya, J., Michaels, A., Subramaniam, A., and Carpenter, E.: New nitrogen input to the tropical North Atlantic Ocean by nitrogen fixation by the cyanobacterium, *Trichodesmium* spp, Global Biogeochem. Cy, 19, 2004.

Capone, D. G., and Carpenter, E. J.: Nitrogen fixation in the marine environment, Science, 217, 1140-1142, 1982.

Capone, D. G., Zehr, J. P., Paerl, H. W., Bergman, B., and Carpenter, E. J.: *Trichodesmium*, a globally significant marine cyanobacterium, Science, 276, 1221-1229, 1997.

Capone, D. G., Subramaniam, A., Montoya, J. P., Voss, M., Humborg, C., Johansen, A. M., Siefert, R. L., and Carpenter, E. J.: An extensive bloom of the N_2-fixing cyanobacterium *Trichodesmium* erythraeum in the central Arabian Sea, Mar. Ecol.-Prog. Ser., 172, 281-292, 1998.

Castruita, M., Saito, M., Schottel, P., Elmegreen, L., Myneni, S., Stiefel, E., and Morel, F. M.: Overexpression and characterization of an iron storage and DNA-binding Dps protein from *Trichodesmium erythraeum*, Applied and environmental microbiology, 72, 2918-2924, 2006.

Chappell, P. D., and Webb, E. A.: A molecular assessment of the iron stress response in the two phylogenetic clades of *Trichodesmium*, Environmental Microbiology, 12, 13-27, 10.1111/j.1462-2920.2009.02026.x, 2010.

Choi, C., and Berges, J.: New types of metacaspases in phytoplankton reveal diverse origins of cell death proteases, Cell death & disease, 4, e490, 2013.

Coleman, M. L., and Chisholm, S. W.: Ecosystem-specific selection pressures revealed through comparative population genomics, Proceedings of the National Academy of Sciences, 107, 18634-18639, 2010.

Cutter, G. A., and Cutter, L. S.: Biogeochemistry of arsenic and antimony in the North Pacific Ocean, Geochemistry, Geophysics, Geosystems, 7, 2006.

Dandonneau, Y., and Gohin, F.: Meridional and seasonal variations of the sea surface chlorophyll concentration in the southwestern tropical Pacific (14 to 32 S, 160 to 175 E), Deep Sea Research Part A. Oceanographic Research Papers, 31, 1377-1393, 1984.

Dowd, S. E., Callaway, T. R., Wolcott, R. D., Sun, Y., McKeehan, T., Hagevoort, R. G., and Edrington, T. S.: Evaluation of the bacterial diversity in the feces of cattle using 16S rDNA bacterial tag-encoded FLX amplicon pyrosequencing (bTEFAP), BMC microbiology, 8, 125, 2008.

Dupouy, C., Neveux, J., Subramaniam, A., Mulholland, M. R., Montoya, J. P., Campbell, L., Capone, D. G., and Carpenter, E. J.: Satellite captures Trichodesmium blooms in the SouthWestern Tropical Pacific., EOS, Trans American Geophysical Union,, 81, 13-16, 2000.

Dupouy, C., Benielli-Gary, D., Neveux, J., Dandonneau, Y., and Westberry, T. K.: An algorithm for detecting *Trichodesmium* surface blooms in the South Western Tropical Pacific, Biogeosciences, 8, 3631-3647, 10.5194/bg-8-3631-2011, 2011.

Dyhrman, S. T., Webb, E., Anderson, D. M., Moffett, J., and Waterbury, J.: Cell-specific detection of phosphorus stress in *Trichodesmium* from the Western North Atlantic, Limnology and Oceanography, 47, 1832-1836, 2002.

Dyhrman, S. T., Chappell, P. D., Haley, S. T., Moffett, J. W., Orchard, E. D., Waterbury, J. B., and Webb, E. A.: Phosphonate utilization by the globally important marine diazotroph *Trichodesmium*, Nature, 439, 68-71, 2006.

Dyhrman, S. T., and Haley, S. T.: Arsenate resistance in the unicellular marine diazotroph *crocosphaera watsonii*, Frontiers in microbiology, 2, 2011.

Edgar, R. C.: UPARSE: highly accurate OTU sequences from microbial amplicon reads, Nature methods, 10, 996-998, 2013.

Engel, A.: The role of transparent exopolymer particles (TEP) in the increase in apparent particle stickiness (alpha) during the decline of a diatom bloom, Journal of Plankton Research, 22, 485-497, 2000.

Evans, C., Malin, G., Mills, G. P., and Wilson, W. H.: Viral infection of *Emiliania huxleyi* (prymnesiophyceae) leads to elevated production of reactive oxygen species, Journal of Phycology, 42, 1040-1047, 2006.

Frydenborg, B. R., Krediet, C. J., Teplitski, M., and Ritchie, K. B.: Temperature-dependent inhibition of opportunistic vibrio pathogens by native coral commensal bacteria, Microbial ecology, 67, 392-401, 2014.

Georgiou, T., Yu, Y.-T., Ekunwe, S., Buttner, M., Zuurmond, A.-M., Kraal, B., Kleanthous, C., and Snyder, L.: Specific peptide-activated proteolytic cleavage of *Escherichia co*li elongation factor Tu, Proceedings of the National Academy of Sciences, 95, 2891-2895, 1998.

Guo, C., and Tester, P. A.: Toxic effect of the bloom-forming *Trichodesmium* sp. (Cyanophyta) to the copepod Acartia tonsa, Natural Toxins, 2, 222-227, 1994.

Hamady, M., Walker, J. J., Harris, J. K., Gold, N. J., and Knight, R.: Error-correcting barcoded primers for pyrosequencing hundreds of samples in multiplex, Nature methods, 5, 235-237, 2008.

Havaux, M., Guedeney, G., Hagemann, M., Yeremenko, N., Matthijs, H. C., and Jeanjean, R.: The chlorophyll-binding protein IsiA is inducible by high light and protects the cyanobacterium *Synechocystis* PCC6803 from photooxidative stress, FEBS letters, 579, 2289-2293, 2005.

Herbland, A., Le Bouteiller, A., and Raimbault, P.: Size structure of phytoplankton biomass in the equatorial Atlantic Ocean, Deep Sea Research Part A. Oceanographic Research Papers, 32, 819-836, 1985.

Hewson, I., Govil, S. R., Capone, D. G., Carpenter, E. J., and Fuhrman, J. A.: Evidence of *Trichodesmium* viral lysis and potential significance for biogeochemical cycling in the oligotrophic ocean, Aquatic Microbial Ecology, 36, 1-8, 2004.

Hewson, I., Poretsky, R. S., Dyhrman, S. T., Zielinski, B., White, A. E., Tripp, H. J., Montoya, J. P., and Zehr, J. P.: Microbial community gene expression within colonies of the diazotroph, *Trichodesmium*, from the Southwest Pacific Ocean, Isme Journal, 3, 1286-1300, 10.1038/ismej.2009.75, 2009.

Hmelo, L. R., Mincer, T. J., and Van Mooy, B. A.: Possible influence of bacterial quorum sensing on the hydrolysis of sinking particulate organic carbon in marine environments, Environmental microbiology reports, 3, 682-688, 2011.

Hmelo, L. R., Van Mooy, B. A. S., and Mincer, T. J.: Characterization of bacterial epibionts on the cyanobacterium *Trichodesmium*, Aquatic Microbial Ecology, 67, 1-U119, 10.3354/ame01571, 2012.

Holmes, R. M., Aminot, A., Kérouel, R., Hooker, B. A., and Peterson, B. J.: A simple and precise method for measuring ammonium in marine and freshwater ecosystems, Canadian Journal of Fisheries and Aquatic Sciences, 56, 1801-1808, 10.1139/f99-128, 1999.

Hove-Jensen, B., Zechel, D. L., and Jochimsen, B.: Utilization of Glyphosate as Phosphate Source: Biochemistry and Genetics of Bacterial Carbon-Phosphorus Lyase, Microbiology and Molecular Biology Reviews, 78, 176-197, 2014.

Hunt, B. P. V., Bonnet, S., Berthelot, H., Conroy, B. J., Foster, R., and Pagano, M.: Contribution and pathways of diazotroph derived nitrogen to zooplankton during the VAHINE mesocosm experiment in the oligotrophic New Caledonia lagoon, This issue.

Ivars-Martinez, E., Martin-Cuadrado, A.-B., D'Auria, G., Mira, A., Ferriera, S., Johnson, J., Friedman, R., and Rodriguez-Valera, F.: Comparative genomics of two ecotypes of the marine planktonic copiotroph *Alteromonas macleodii* suggests alternative lifestyles associated with different kinds of particulate organic matter, The ISME journal, 2, 1194-1212, 2008.

Jacquet, S., Heldal, M., Iglesias-Rodriguez, D., Larsen, A., Wilson, W., and Bratbak, G.: Flow cytometric analysis of an *Emiliana huxleyi* bloom terminated by viral infection, Aquatic Microbial Ecology, 27, 111-124, 2002.

Jacquet, S., Delesalle, B., Torréton, J.-P., and Blanchot, J.: Response of phytoplankton communities to increased anthropogenic influences (southwestern lagoon, New Caledonia), Marine Ecology Progress Series, 320, 65-78, 2006.

Jeanjean, R., Zuther, E., Yeremenko, N., Havaux, M., Matthijs, H. C., and Hagemann, M.: A photosystem 1 *psaFJ*-null mutant of the cyanobacterium *Synechocystis* PCC 6803 expresses the *isiAB* operon under iron replete conditions, FEBS letters, 549, 52-56, 2003.

Kerbrat, A.-S., Darius, H. T., Pauillac, S., Chinain, M., and Laurent, D.: Detection of ciguatoxin-like and paralysing toxins in *Trichodesmium* spp. from New Caledonia lagoon, Marine pollution bulletin, 61, 360-366, 2010.

Kopylova, E., Noé, L., and Touzet, H.: SortMeRNA: fast and accurate filtering of ribosomal RNAs in metatranscriptomic data, Bioinformatics, 28, 3211-3217, 2012.

Kustka, A., Carpenter, E. J., and Sañudo-Wilhelmy, S. A.: Iron and marine nitrogen fixation: progress and future directions, Research in Microbiology, 153, 255-262, 2002.

La Roche, J., Boyd, P. W., McKay, R. M. L., and Geider, R. J.: Flavodoxin as an in situ marker for iron stress in phytoplankton, Nature, 382, 802-805, 1996.

Langmead, B., and Salzberg, S. L.: Fast gapped-read alignment with Bowtie 2, Nature methods, 9, 357-359, 2012.

Latham, M.: Aptitudes culturales et forestières. ln" Atlas de la Nouvelle-Calédonie et dépendances, Editions ORSTOM, 1981.

Latifi, A., Jeanjean, R., Lemeille, S., Havaux, M., and Zhang, C.-C.: Iron starvation leads to oxidative stress in *Anabaena* sp. strain PCC 7120, Journal of bacteriology, 187, 6596-6598, 2005.

Laudenbach, D. E., and Straus, N. A.: Characterization of a cyanobacterial iron stress-induced gene similar to psbC, Journal of bacteriology, 170, 5018-5026, 1988.

Leblanc, K., Cornet, V., Caffin, M., Rodier, M., Desnues, A., Berthelot, H., Heliou, J., and Bonnet, S.: Phytoplankton community structure in the VAHINE mesocosm experiment, This issue.

Lehahn, Y., Koren, I., Schatz, D., Frada, M., Sheyn, U., Boss, E., Efrati, S., Rudich, Y., Trainic, M., and Sharoni, S.: Decoupling physical from biological processes to assess the impact of viruses on a mesoscale algal bloom, Current Biology, 24, 2041-2046, 2014.

Leonhardt, K., and Straus, N. A.: An iron stress operon involved in photosynthetic electron transport in the marine cyanobacterium *Synechococcus* sp. PCC 7002, Journal of general microbiology, 138, 1613-1621, 1992.

Luo, Y.-W., Doney, S., Anderson, L., Benavides, M., Berman-Frank, I., Bode, A., Bonnet, S., Boström, K., Böttjer, D., and Capone, D.: Database of diazotrophs in global ocean: abundance, biomass and nitrogen fixation rates, Earth System Science Data, 4, 47-73, 2012.

Mackey, K. R., Post, A. F., McIlvin, M. R., Cutter, G. A., John, S. G., and Saito, M. A.: Divergent responses of Atlantic coastal and oceanic *Synechococcus* to iron limitation, Proceedings of the National Academy of Sciences, 112, 9944-9949, 2015.

Martin, M.: Cutadapt removes adapter sequences from high-throughput sequencing reads, EMBnet. journal, 17, pp. 10-12, 2011.

Martinez, A., Tyson, G. W., and DeLong, E. F.: Widespread known and novel phosphonate utilization pathways in marine bacteria revealed by functional screening and metagenomic analyses, Environmental Microbiology, 12, 222-238, 10.1111/j.1462-2920.2009.02062.x, 2010.

Massana, R., Murray, A. E., Preston, C. M., and DeLong, E. F.: Vertical distribution and phylogenetic characterization of marine planktonic Archaea in the Santa Barbara Channel, Applied and environmental microbiology, 63, 50-56, 1997.

Michel, K. P., and Pistorius, E. K.: Adaptation of the photosynthetic electron transport chain in cyanobacteria to iron deficiency: the function of IdiA and IsiA, Physiologia Plantarum, 120, 36-50, 2004.

Mohr, W., Grosskopf, T., Wallace, D. W., and LaRoche, J.: Methodological underestimation of oceanic nitrogen fixation rates, PLOS one, 5, e12583, 2010.

Montoya, J. P., Voss, M., Kahler, P., and Capone, D. G.: A simple, high-precision, high-sensitivity tracer assay for N_2 fixation, Applied and Environmental Microbiology, 62, 986-993, 1996.

Moutin, T., Van Den Broeck, N., Beker, B., Dupouy, C., Rimmelin, P., and Le Bouteiller, A.: Phosphate availability controls *Trichodesmium* spp. biomass in the SW Pacific Ocean, Mar. Ecol.-Prog. Ser., 297, 15-21, 2005.

Mulholland, M. R., and Capone, D. G.: The nitrogen physiology of the marine N_2-fixing cyanobacteria *Trichodesmium* spp, Trends Plant Sci., 5, 148-153, 2000.

Mulholland, M. R.: The fate of nitrogen fixed by diazotrophs in the ocean, Biogeosciences, 4, 37-51, 2007.

O'Neil, J. M., and Roman, M. R.: Ingestion of the Cyanobacterium *Trichodesmium* spp by Pelagic Harpacticoid Copepods *Macrosetella*, *Miracia* and *Oculostella*, Hydrobiologia, 293, 235-240, 1994.

O'Neil, J. M.: The colonial cyanobacterium *Trichodesmium* as a physical and nutritional substrate for the harpacticoid copepod *Macrosetella gracilis*, Journal of Plankton Research, 20, 43-59, 1998.

Ohki, K.: A possible role of temperate phage in the regulation of *Trichodesmium* biomass, Bulletin de l'institute oceanographique, Monaco, 19, 287-291, 1999.

Orchard, E., Webb, E., and Dyhrman, S.: Characterization of phosphorus-regulated genes in *Trichodesmium* spp., The Biological Bulletin, 205, 230-231, 2003.

Paerl, H. W., Priscu, J. C., and Brawner, D. L.: Immunochemical localization of nitrogenase in marine *Trichodesmium* aggregates: Relationship to N_2 fixation potential, Applied and environmental microbiology, 55, 2965-2975, 1989.

Passow, U., and Alldredge, A. L.: A dye binding assay for the spectrophotometeric measurement of transparent exopolymer particles (TEP), Limnol. & Oceanogr, 40, 1326-1335, 1995.

Pfreundt, U., Kopf, M., Belkin, N., Berman-Frank, I., and Hess, W. R.: The primary transcriptome of the marine diazotroph *Trichodesmium erythraeum* IMS101, Sci. Rep., 4, 2014.

Pfreundt, U., Van Wambeke, F., Bonnet, S., and Hess, W. R.: Comparative analysis of the prokaryotic community in the New Caledonia lagoon and within the VAHINE mesocosms experiment, an experimental ecosystem challenge This issue.

Pichon, D., Cudennec, B., Huchette, S., Djediat, C., Renault, T., Paillard, C., and Auzoux-Bordenave, S.: Characterization of abalone *Haliotis tuberculata–Vibrio harveyi* interactions in gill primary cultures, Cytotechnology, 65, 759-772, 2013.

Pujo-Pay, M., and Raimbault, P.: Improvement of the wet-oxidation procedure for simultaneous determination of particulate organic nitrogen and phosphorus collected on filters, Mar. Ecol.-Prog. Ser., 105, 203–207, 10.3354/meps105203, 1994.

Quast, C., Pruesse, E., Yilmaz, P., Gerken, J., Schweer, T., Yarza, P., Peplies, J., and Glöckner, F. O.: The SILVA ribosomal RNA gene database project: improved data processing and web-based tools, Nucleic Acids Research, 41, D590-D596, 10.1093/nar/gks1219, 2013.

Rahav, E., Herut, B., Levi, A., Mulholland, M., and Berman-Frank, I.: Springtime contribution of dinitrogen fixation to primary production across the Mediterranean Sea, Ocean Science, 9, 489-498, 2013.

Rodier, M., and Le Borgne, R.: Population dynamics and environmental conditions affecting *Trichodesmium* spp. (filamentous cyanobacteria) blooms in the south-west lagoon of New Caledonia, Journal of Experimental Marine Biology and Ecology, 358, 20-32, 10.1016/j.jembe.2008.01.016, 2008.

Rodier, M., and Le Borgne, R.: Population and trophic dynamics of *Trichodesmium thiebautii* in the SE lagoon of New Caledonia. Comparison with *T. erythraeum* in the SW lagoon, Marine Pollution Bulletin, 61, 349-359, 2010.

Sheridan, C. C., Steinberg, D. K., and Kling, G. W.: The microbial and metazoan community associated with colonies of *Trichodesmium* spp.: a quantitative survey, Journal of Plankton Research, 24, 913-922, 2002.

Siddiqui, P. J., Bergman, B., Bjorkman, P. O., and Carpenter, E. J.: Ultrastructural and chemical assessment of poly-beta-hydroxybutyric acid in the marine cyanobacterium *Trichodesmium thiebautii*, FEMS Microbiology Letters, 73, 143-148, 1992.

Smetacek, V.: Role of sinking in diatom life-history cycles: ecological, evolutionary and geological significance, Marine biology, 84, 239-251, 1985.

Spungin, D., Berman-Frank, I., and Levitan, O.: *Trichodesmium's* strategies to alleviate phosphorus limitation in the future acidified oceans, Environmental microbiology, 16, 1935-1947, 2014.

Spungin, D., Elifantz, H., Rosenberg, G., Bidle, K. D., and Berman-Frank, I.: Metacaspases and bloom demise in the marine cyanobacterium *Trichodesmium*, In prep.

Strickland, J. D. H., and Parsons, T. R.: A Practical Handbook of Seawater Analysis, Fisheries Research Board of Canada, Ottawa, 1972.

Tandeau de Marsac, N., and Houmard, J.: Complementary chromatic adaptation: Physiological conditions and action spectra, in: Methods in Enzymology, Academic Press, 318-328, 1988.

Tarutani, K., Nagasaki, K., and Yamaguchi, M.: Viral impacts on total abundance and clonal composition of the harmful bloom-forming phytoplankton heterosigma akashiwo, Applied and Environmental Microbiology, 66, 4916-4920, 2000.

Thamatrakoln, K., Korenovska, O., Niheu, A. K., and Bidle, K. D.: Whole-genome expression analysis reveals a role for death-related genes in stress acclimation of the diatom *Thalassiosira pseudonana*, Environmental microbiology, 14, 67-81, 2012.

Turk-Kubo, K., Frank, I., Hogan, M., Desnues, A., Bonnet, S., and Zehr, J.: Diazotroph community succession during the VAHINE mesocosms experiment (New Caledonia Lagoon), Biogeosciences Discussions, 12, 9043–9079, 2015.

Van Mooy, B. A., Hmelo, L. R., Sofen, L. E., Campagna, S. R., May, A. L., Dyhrman, S. T., Heithoff, A., Webb, E. A., Momper, L., and Mincer, T. J.: Quorum sensing control of phosphorus acquisition in *Trichodesmium* consortia, The ISME journal, 6, 422-429, 2012.

Van Wambeke, F., Pfreundt, U., Moutin, T., Rodier, M., Berthelot, H., and Bonnet, S.: Dynamics of heterotrophic bacterial community during an experimental diazotrophic bloom in New Caledonia and links with transcriptional changes during the VAHINE mesocosms experiment, Biogeosciences Discussions, This issue.

Vardi, A., Berman-Frank, I., Rozenberg, T., Hadas, O., Kaplan, A., and Levine, A.: Programmed cell death of the dinoflagellate *Peridinium gatunense* is mediated by CO_2 limitation and oxidative stress, Current Biology: CB, 9, 1061-1064, 1999.

Vardi, A., Haramaty, L., Van Mooy, B. A., Fredricks, H. F., Kimmance, S. A., Larsen, A., and Bidle, K. D.: Host–virus dynamics and subcellular controls of cell fate in a natural coccolithophore population, Proceedings of the National Academy of Sciences, 109, 19327-19332, 2012.

Walsby, A. F.: The properties and bouyancy providing role of gas vacuoles in *Trichodesmium*, Ehrenberg. Br. Phycol. J., 13, 103-116, 1978.

Wu, Z., Jenkins, B. D., Rynearson, T. A., Dyhrman, S. T., Saito, M. A., Mercier, M., and Whitney, L. P.: Empirical bayes analysis of sequencing-based transcriptional profiling without replicates, BMC bioinformatics, 11, 564, 2010.

Biogeosciences Discuss., doi:10.5194/bg-2015-613, 2016
Manuscript under review for journal Biogeosciences
Published: 18 January 2016

Zehr, J. P.: Nitrogen fixation in the Sea: Why Only *Trichodesmium*, in: Molecular Ecology of Aquatic Microbes, edited by: Joint, I., NATO ASI Series, Springer-Verlag, Heidelberg, 335-363, 1995.

Biogeosciences Discuss., doi:10.5194/bg-2015-613, 2016
Manuscript under review for journal Biogeosciences
Published: 18 January 2016

Figure legends

Figure 1. Temporal dynamics of depth-averaged Chl *a* concentrations (µg L^{-1}) in the lagoon waters outside the VAHINE mesocosms throughout the experimental period from day 2 to 23. The increase in Chl *a*. for day 23 represents an increase in *Trichodesmium* as well as other photosynthetic organisms present in the lagoon at the time (Van Wambeke et al., This issue; Leblanc et al., This issue).

Figure 2. (a-c) Dense surface blooms of *Trichodesmium* observed outside the mesocosms in the lagoon waters on day 23 at 12:00 and 17:00. Photos illustrate the spatial heterogeneity of the surface accumulations and the high density of the biomass. (d-e) To examine the mechanistic of demise, *Trichodesmium* biomass was subsampled from the surface populations, resuspended in filtered seawater in 6 4.6 L^{-1} bottles, and incubated on-deck in running-seawater pools with ambient surface temperature (~ 26 °C) at 50 % of the surface irradiance. Bottles were sampled every 2-4 h for different parameters until the biomass crashed. (f) Temporal changes in Chl *a* concentrations in the bottles from the time of biomass collection and resuspension in the bottles until the *Trichodesmium* biomass crashed ~ 24 h after the experiment began (average n=3-6). Photo c. courtesy of A. Renaud.

Figure 3. Particulate organic nitrogen (PON) (µmol L^{-1}) and N_2 fixation rates (nmol L^{-1} h^{-1}) during (a) pre-bloom days (d 2-23) and during (b) the *Trichodesmium* surface accumulation (bloom) and demise (d 23-25), short-term experiment 2. NH_4^+ concentration (nmol L^{-1}) during (c) pre-bloom days (d 2-23) and during (d) the *Trichodesmium* surface accumulation (bloom) and demise (d 23-25), short-term experiment 2.

Figure 4. Dynamics of microbial community abundance and diversity during *Trichodesmium* surface bloom as obtained by 16S rRNA gene sequencing for samples collected from the surface waters outside the mesocosms during *Trichodesmium* surface accumulation (bloom) (short-term experiment 1). Pie charts show the changes in dominant groups during the *Trichodesmium* bloom and crash from two replicate incubation bottles. The graphs below show the respective temporal dynamics of *Trichodesmium* (white circles) and *Alteromonas* (gray triangles), the dominant bacterial species during the bloom crash.

Figure 5. Virus like particles (VLP mL^{-1} x 10^6)**,** Particulate organic nitrogen (PON) and Particulate organic carbon (POC) during (a) pre-bloom days (d 2-23) and during (b) *Trichodesmium* surface accumulation (bloom) and demise (d 23-24) (short-term experiment

Biogeosciences Discuss., doi:10.5194/bg-2015-613, 2016
Manuscript under review for journal Biogeosciences
Published: 18 January 2016

2). Standard error for technical replicates (VLP) (n=3) was < 1 %, which is smaller than symbol size.

Figure 6. (a) Expression of alkaline phosphatase associated genes *phoA and phoX* (Tery_3467 and Tery_3845) and phosphonate utilization genes (*phn* genes, Tery_0365*, Tery_0366*, Tery_0367*, Tery_4993, Tery_4994, Tery_4995, Tery_4996*, Tery_4997, Tery_4998, Tery_4999, Tery_5000, Tery_5001 Tery_5002 and Tery_5003). Asterisks near locus tag numbers indicate gene duplicates. (b) Iron-related genes, *isiB* (Tery_1666), *isiA* (Tery_1667), *idiA* (Tery_3377), and ferritin *DPS* gene *dpsA* (Tery_4282). Bars represent RNA-Seq read counts normalized as reads per million reads (RPM) mapped to the *T. erythraeum* IMS101 genome at three time points: T_0 (peak of the bloom), T_8 (eight hours after T_0) and T_{22} (22 hours since T_0). Significant expression was tested with ASC (Wu et al., 2010) and marked with an asterisk. Black asterisks represent significant change from T_0 and red asterisks represent significant change from T_8. A gene was called differentially expressed if P > 0.98 (posterior probability).

Figure 7. Dynamics of caspase specific activity rates (pmol L^{-1} min^{-1}) of *Trichodesmium* in the New Caledonia lagoon (a) during pre-bloom days and (b) during bloom accumulation and bloom demise, sampled during a short-term incubation experiment. Samples (n=3-6) collected from the bloom (day 23, 12:00 T_0), were incubated on-deck in an incubator fitted with running seawater to maintain ambient surface temperature (~ 26 °C). (c). Transcript accumulation of metacaspase genes in the *Trichodesmium* bloom during the short-term incubation experiment. Metacaspase genes are *TeMC1* (Tery_2077), *TeMC2* (Tery_2689), *TeMC3* (Tery_3869), *TeMC4* (Tery_2471), *TeMC5* (Tery_2760), *TeMC6* (Tery_2058), *TeMC7* (Tery_1841), *TeMC8* (Tery_0382), *TeMC9* (Tery_4625), *TeMC10* (Tery_2624), *TeMC11* (Tery_2158) and *TeMC12* (Tery_2963). Bars represent RNA-Seq read counts normalized as reads per million reads (RPM) mapped to the *T. erythraeum* IMS101 genome at three time points: T_0 (peak of the bloom), T_8 (8 hours after T_0) and T_{22} (22 hours since T_0). Significant expression was tested with ASC (Wu et al., 2010) and marked with an asterisk. Black asterisks represent significant change from T_0 and red asterisks represent significant change from T_8. A gene was called differentially expressed if P > 0.98 (posterior probability).

Figure 8. Changes in the concentrations of transparent exopolymer particles (TEP) (µg GX L^{-1}) and particulate organic carbon (POC) (µmol L^{-1}) during (a) pre-bloom days (days 2-23)

Biogeosciences Discuss., doi:10.5194/bg-2015-613, 2016
Manuscript under review for journal Biogeosciences
Published: 18 January 2016

sampled from the surrounding lagoon waters (OUT) at 1m depth (surface) (n=3). And (b) during bloom accumulation and demise, short-term-experiment 2 (n=3).

Figure 9. Transcript accumulation of gas vesicle protein (gvp) genes as obtained from metatranscriptomic analyses of the *Trichodesmium* bloom from peak to collapse (days 23-24). *gvpA* genes (Tery_2330 and Tery_2335*) encode the main constituent of the gas vesicles that forms the essential core of the structure; *gvpN* (Tery_2329 and Tery_2334) *gvpK* (Tery_2322), *gvpG* (Tery_2338) and *gvpL/gvpF* (Tery_2339 and Tery_2340*) encode vesicle synthesis proteins. Bars represent RNA-Seq read counts normalized as reads per million reads (RPM) mapped to the *T. erythraeum* IMS101 genome at 3 time points: T_0 (peak of the bloom), T_8 (8 hours after T_0) and T_{22} (22 hours after T_0). Significant expression of at least 2-fold was tested with ASC (Wu et al., 2010) and is marked with an asterisk. Black asterisks represent significant change from T_0 and red asterisks represent significant changes from T_8. A gene was defined as differentially expressed if P > 98 (posterior probability).

Biogeosciences Discuss., doi:10.5194/bg-2015-613, 2016
Manuscript under review for journal Biogeosciences
Published: 18 January 2016

Figure 1

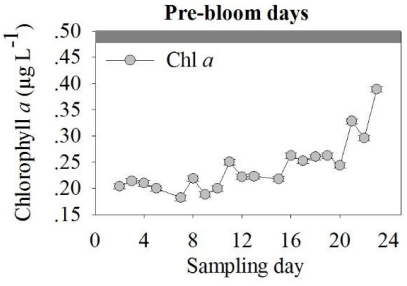

Biogeosciences Discuss., doi:10.5194/bg-2015-613, 2016
Manuscript under review for journal Biogeosciences
Published: 18 January 2016

Figure 2

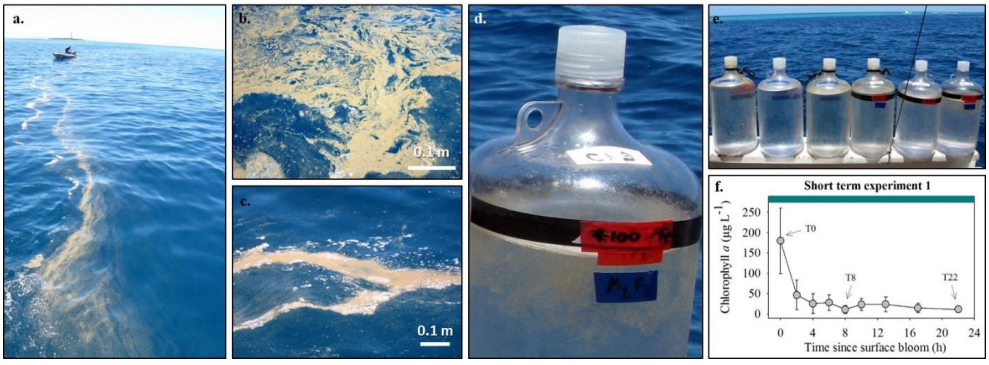

Biogeosciences Discuss., doi:10.5194/bg-2015-613, 2016
Manuscript under review for journal Biogeosciences
Published: 18 January 2016

Figure 3

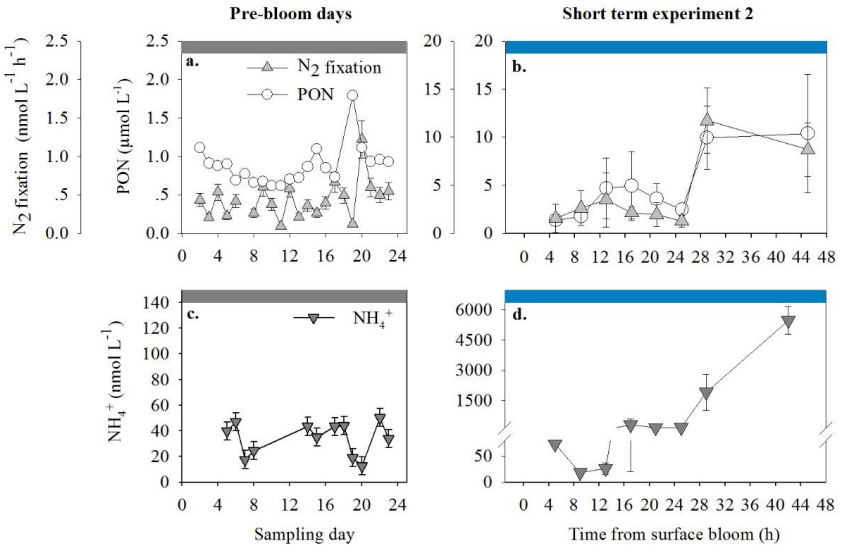

Biogeosciences Discuss., doi:10.5194/bg-2015-613, 2016
Manuscript under review for journal Biogeosciences
Published: 18 January 2016

Figure 4

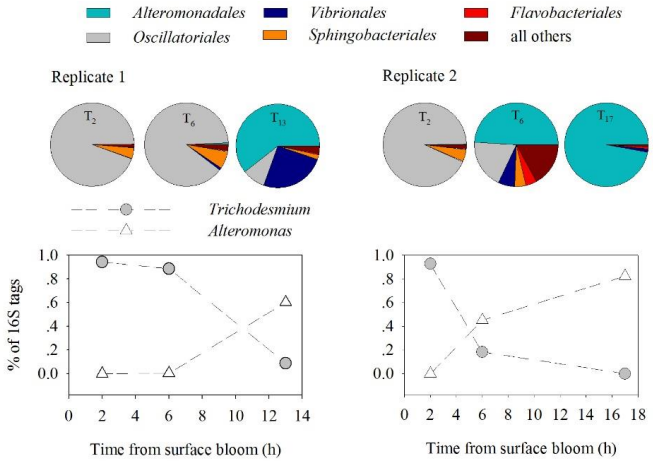

Biogeosciences Discuss., doi:10.5194/bg-2015-613, 2016
Manuscript under review for journal Biogeosciences
Published: 18 January 2016

Figure 5

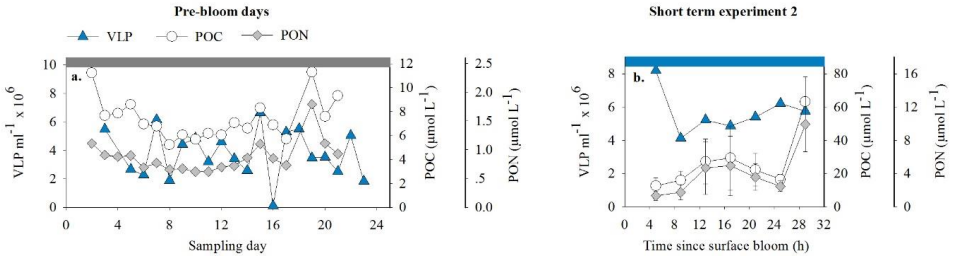

Biogeosciences Discuss., doi:10.5194/bg-2015-613, 2016
Manuscript under review for journal Biogeosciences
Published: 18 January 2016

Figure 6

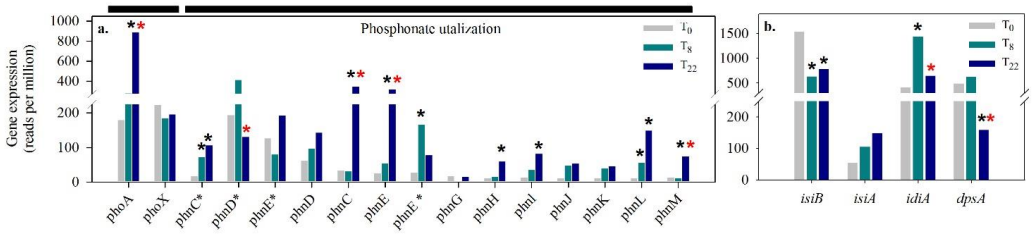

Biogeosciences Discuss., doi:10.5194/bg-2015-613, 2016
Manuscript under review for journal Biogeosciences
Published: 18 January 2016

Figure 7

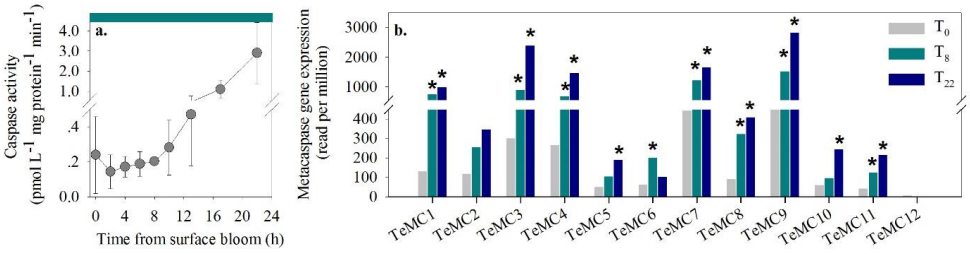

Biogeosciences Discuss., doi:10.5194/bg-2015-613, 2016
Manuscript under review for journal Biogeosciences
Published: 18 January 2016

Figure 8

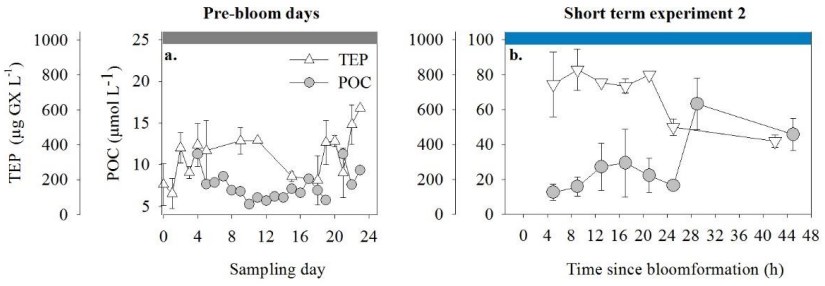

Biogeosciences Discuss., doi:10.5194/bg-2015-613, 2016
Manuscript under review for journal Biogeosciences
Published: 18 January 2016

Figure 9